Title

Using line acceleration to measure false killer whale (Pseudorca crassidens) click and whistle source levels during pelagic longline depredation

Journal

The Journal of the Acoustical Society of America, 140(5)

ISSN

0001-4966

Authors

Thode, Aaron
Wild, Lauren
Straley, Janice
et al.

Publication Date

2016-11-01

DOI

10.1121/1.4966625

Peer reviewed

Using line acceleration to measure false killer whale (*Pseudorca crassidens*) click and whistle source levels during pelagic longline depredation

Aaron Thode[a)]
Marine Physical Laboratory, Scripps Institution of Oceanography, University of California San Diego, La Jolla, California 92093-0238, USA

Lauren Wild
Sitka Sound Science Center, 8340 Lincoln Street, Sitka, Alaska 99835, USA

Janice Straley
University of Alaska Southeast, 1332 Seward Avenue, Sitka, Alaska 99835, USA

Dustin Barnes
National Oceanic and Atmospheric Administration Fisheries Pacific Islands Regional Office Observer Program, 1845 Wasp Boulevard, Building 176, Honolulu, Hawaii 96818, USA

Ali Bayless
Joint Institute for Marine & Atmospheric Research, University of Hawaii at Manoa, affiliated with National Oceanic and Atmospheric Administration Fisheries Pacific Islands Fisheries Science Center, 1845 Wasp Boulevard, Building 176, Honolulu, Hawaii 96818, USA

Victoria O'Connell
Sitka Sound Science Center, 8340 Lincoln Street, Sitka, Alaska 99835, USA

Erin Oleson
National Oceanic and Atmospheric Administration Fisheries Pacific Islands Fisheries Science Center, 1845 Wasp Boulevard, Building 176, Honolulu, Hawaii 96818, USA

Jit Sarkar
Marine Physical Laboratory, Scripps Institution of Oceanography, University of California San Diego, La Jolla, California 92093-0238, USA

Dan Falvey and Linda Behnken
Alaska Longline Fishermen's Association, P.O. Box 1229, Sitka, Alaska 99835, USA

Sean Martin
POP Fishing & Marine, 1133 North Nimitz Highway, Honolulu, Hawaii 96817, USA

(Received 16 March 2016; revised 14 October 2016; accepted 18 October 2016; published online 22 November 2016)

False killer whales (*Pseudorca crassidens*) depredate pelagic longlines in offshore Hawaiian waters. On January 28, 2015 a depredation event was recorded 14 m from an integrated GoPro camera, hydrophone, and accelerometer, revealing that false killer whales depredate bait and generate clicks and whistles under good visibility conditions. The act of plucking bait off a hook generated a distinctive 15 Hz line vibration. Two similar line vibrations detected at earlier times permitted the animal's range and thus signal source levels to be estimated over a 25-min window. Peak power spectral density source levels for whistles (4–8 kHz) were estimated to be between 115 and 130 dB re 1 μPa^2/Hz @ 1 m. Echolocation click source levels over 17–32 kHz bandwidth reached 205 dB re 1 μPa @ 1 m pk-pk, or 190 dB re 1 μPa @ 1 m (root-mean-square). Predicted detection ranges of the most intense whistles are 10 to 25 km at respective sea states of 4 and 1, with click detection ranges being 5 times smaller than whistles. These detection range analyses provide insight into how passive acoustic monitoring might be used to both quantify and avoid depredation encounters. © *2016 Acoustical Society of America*. [http://dx.doi.org/10.1121/1.4966625]

[JFL] Pages: 3941–3951

I. INTRODUCTION AND BACKGROUND

A. False killer whale depredation of pelagic longlines

False killer whales (*Pseudorca crassidens*), abbreviated FKWs here, are found in tropical and warm-temperate waters throughout the world. The species has been implicated in removing catch, or depredating, from pelagic fisheries in several regions around the world (Gilman *et al.*, 2007). This depredation can occasionally result in the whale becoming hooked or entangled in fishing gear, and almost always results in a financial loss to the fishermen. There have been a number of attempts to deter FKWs from taking catch from fishing gear, though few have met with prolonged success.

[a)]Electronic mail: athode@ucsd.edu

Depredation of bigeye tuna and other large pelagic fish by FKWs is a chronic concern within the Hawaii-based pelagic deep-set longline fishery. Three different stocks of FKWs are recognized in Hawaiian waters: the Main Hawaiian Islands (MHIs) insular stock, the Northwestern Hawaiian Islands (NWHIs) stock, and the Hawaii pelagic stock (Carretta *et al.*, 2016). The MHI insular and NWHI stocks primarily occur within regions closed to longline fishing, though depredation and bycatch of those stocks is still possible within this fishery in certain regions. The Hawaii pelagic population of FKWs is largely responsible for depredation of catch, and is also most frequently bycaught when they become hooked or entangled in gear. The minimum population size of the pelagic population within the Hawaiian Exclusive Economic Zone (EEZ), estimated from transect surveys, is 928 animals, corresponding to a Potential Biological Removal (PBR), or sustainable take rate, of 9.3 animals per year. The number of pelagic FKWs seriously injured or killed due to hooking or entanglement in the Hawaii-based longline fishery has exceeded this sustainable level since at least the late 1990s (Carretta *et al.*, 2016), and is therefore considered a "strategic" stock under the U.S. Marine Mammal Protection Act. The minimum size of the MHI insular population of FKWs is much smaller (92 individuals from photo-identification studies), and corresponding PBR of 0.2 animals per year, such that even very low levels of bycatch within the longline fishery are of concern for this population. The MHI insular population is designated as endangered under U.S. Endangered Species Act of 1971 (November 2012 77 FR 70915).

Hawaii hosts both deep- and shallow-set pelagic longline fisheries. The offshore deep-set fishery is conducted by setting 40–60 km of 3.5 mm monofilament "mainline" deployed at depths between 50 and 400 m (Fig. 1). At various intervals "branch lines" are clipped to the mainline using detachable snaps, with the other end of the branchline terminating in a hook. The target catch of the deep-set fishery is bigeye tuna, but bycatch species include sharks, turtles, and marine mammals such as pilot whales and FKWs (Bradford and Forney, 2016; Gilman *et al.*, 2007; Hamer *et al.*, 2012; Watson and Kerstetter, 2006). Sets require several hours to deploy, and then require between 10 and 15 h of hauling, with the last end deployed typically being the first to be hauled.

Between 2009 and 2013 National Marine Fisheries Service (NMFS) fisheries observers noted 24 FKWs, later judged to be seriously injured or killed, due to hooking or entanglement in the Hawaii-based deep-set longline (Carretta *et al.*, 2016). During this same period five other unidentified cetaceans, possibly FKWs, were also seriously injured or killed. Once accounting for the distribution of fishing effort and the level of observer coverage, the minimum bycatch estimate within the Hawaiian EEZ is approximately 11 pelagic FKWs per year (Carretta *et al.*, 2016). The rate is much lower for MHI insular and NWHI FKWs. As a result of long-term unsustainable rates of bycatch within the Hawaii-based longline fishery, in January 2010 the NMFS established a Take Reduction Team to develop strategies to reduce incidental mortality and serious injury of this species to below PBR. The resulting Take Reduction Plan (TRP) became effective on December 31, 2012, and incorporates "gear requirements, time-area closures, and measures to improve captain and crew response to hooked and entangled whales" (November 2012 77 FR 71260).

Although the TRP has enacted measures that aim to reduce bycatch rates for pelagic FKWs, many aspects of the mechanics of depredation and gear interactions remain unknown, due to the difficulties of conducting direct observations of depredation far offshore Hawaii. For example, at the start of the study it was unknown whether FKWs targeted bait as well as catch species. Were animals to target bait, the scale of potential interactions with gear increases substantially.

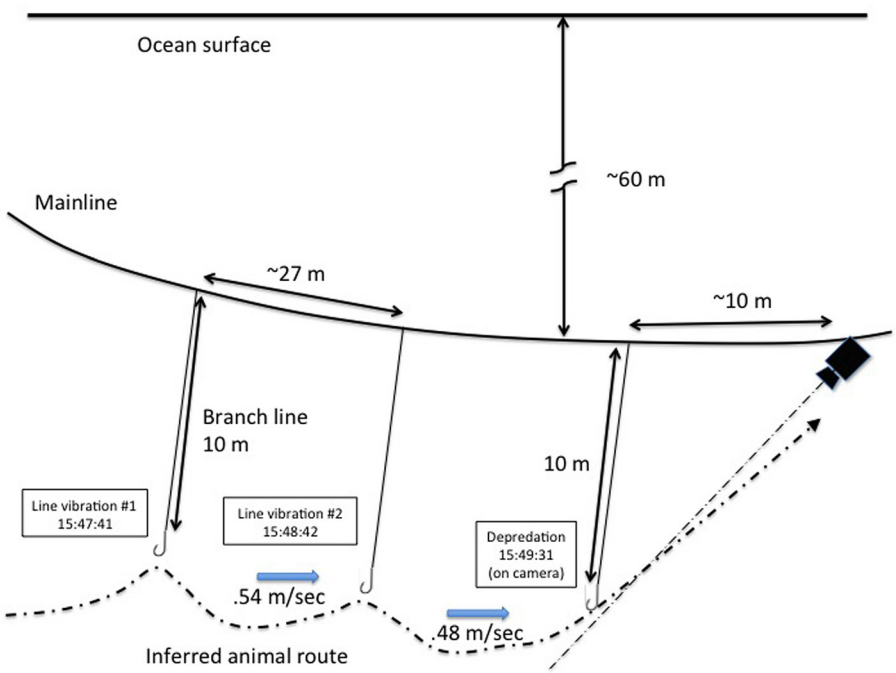

FIG. 1. (Color online) Illustration of experimental configuration on pelagic longline used to estimate source levels. The dashed-dotted line indicates the FKW's estimated route, inferred from both accelerometer and video data.

B. FKW acoustics

Another unknown aspect of depredation was the degree to which FKWs use sound during various stages of depredation. FKWs generate both relatively low-frequency whistles (4–10 kHz) (Oswald *et al.*, 2003) and ultrasonic clicks (20–120 kHz). Clicks, often generated in sets that will be defined here as "buzzes" or "bursts," are known to serve as echolocation signals (Thomas *et al.*, 1988; Brill *et al.*, 1992; Au *et al.*, 1995; Baumann-Pickering *et al.*, 2015), while whistles are believed to serve as some sort of communication/social cohesion role, analogous with other odontocete species. The NMFS Pacific Islands Fisheries Science Center has been deploying passive acoustic recorders on longlines to quantify FKW encounter rates (Bayless *et al.*, 2017). However, at the time the program began it was unknown whether animals use acoustics to depredate under good visual conditions, or whether they use vision exclusively in such circumstances.

On a more fundamental level, the range over which passive acoustics could detect depredating animals was unknown, because the source levels of both whistles and clicks were relatively unknown. The only study to measure click source levels from free-ranging FKWs obtained values between 201 and 225 dB re 1 μPa (pk-pk) for "on-axis" measurements made within the beam of the animals' sonar, but did not publish values for "off-axis" measurements that would be more representative for distant passive acoustic detections (Madsen *et al.*, 2004). Several other papers have been published on the on-axis source levels from captive animals (Thomas *et al.*, 1988; Brill *et al.*, 1992; Au *et al.*, 1995; Kloepper *et al.*, 2012), but have generally yielded lower source levels than Madsen *et al.* (2004), raising questions about how applicable the results are to field conditions.

The measured spectra of clicks vary depending on whether measured in the field or captivity. Restricting the review to field measurements, Madsen *et al.* (2004) observed on-axis bimodal spectra with peak frequencies around 40–60 kHz, while other measurements of more distant clicks at unknown ranges noted broad peaks around 22 kHz (Baumann-Pickering *et al.*, 2015). The differences in these results likely arise from the signals' directivity and the fact that the frequency content of a click will shift downward with increasing propagation distance, due to the relatively higher attenuation of higher frequency components when propagating through ocean water.

This study describes how 14 commercial pelagic longline sets were instrumented with five integrated camera, hydrophone, and accelerometer packages during a January 2015 trip. Two of these sets each recorded a FKW depredation event, demonstrating that the animals depredate bait and that they generate whistles and clicks while depredating in daylight conditions. Furthermore, the ability to visually identify the animal's position when it was producing sounds, combined with line vibration data logged on the accelerometer, permitted the range of one animal from the camera to be estimated over a 25 min window, which in turn enabled source level estimates of the animal's whistles and of its off-axis band limited echolocation clicks. These source levels are then used to model the theoretical detection range of FKW whistles and clicks recorded for different sea states in deep waters off Hawaii. The resulting simulations provide insight into both the possibilities and limitations of using passive acoustics to detect the presence of FKWs before and during longline deployments.

II. METHODS

A. Equipment

Data were collected on autonomous video/acoustic/accelerometer packages dubbed "TadPros." The heart of the package is a GoPro Hero 3+ Black camera (San Mateo, CA), encased in a commercial "ScoutPro"^{TM} pressure case (GroupInc, Jensen Beach, FL, www.groupbinc.com). An HTI-96 min hydrophone (High Tech Inc., Long Beach, MS) with −172 dB re V/1 μPa sensitivity is attached to the end of the case via a five-pin Subconn connector. When powered by an external 7.2 V 2300 mAh NiMh battery pack, the GoPro can record up to 5 h of video and stereo audio continuously to an internal microSD card.

While conveniently sized with reasonable video quality, the GoPro has relatively poor audio specifications. The camera has an external mini-USB port that accepts external stereo audio input, but the internal bandwidth of the signal is limited to 24 kHz, and the data are stored in a lossy compressed MP4 format. More problematic is that the camera has an internal automatic gain control that makes signal calibration difficult. A final limitation is that the camera's internal software does not include a wake-up timer, a necessary requirement given that several hours can elapse between when a camera is programmed and when it should begin recording underwater.

A custom circuit board [Fig. 2(a)] circumvented these limitations by implementing a field-programmable countdown activation timer, processing external acoustic signals, and logging accelerometer data. The 4 × 6 cm circuit board plugs into the rear dock connector of the camera and uses an

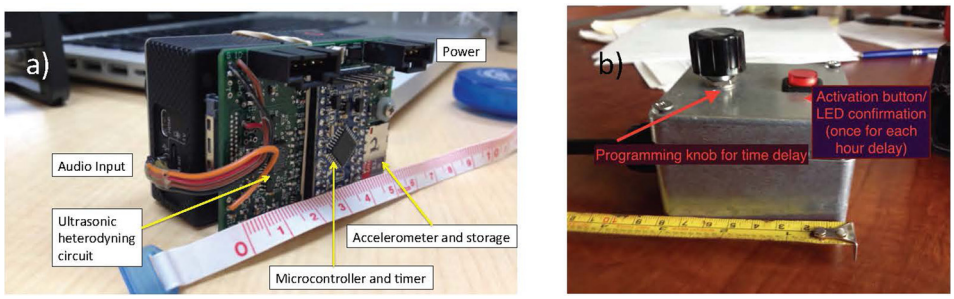

FIG. 2. (Color online) "TadPro" instrument package. (a) Overview of circuit board; (b) external programming box, allowing timing circuit to be reset and adjusted without opening pressure case.

Arduino Pro Mini microcontroller (SparkFun Electronics, Niwot, CO) to perform the timing function and to record accelerometer data to a dedicated MicroSD card. The Arduino controller also generates a 16 kHz local oscillator frequency that drives a double-balanced mixer, and a 14 kHz pilot signal that is mixed with hydrophone audio to serve as reference signal for calibration purposes.

A custom programming box sets the delay timer by connecting through the Subconn connector [Fig. 2(b)]. Rotating a dial on the programming box adjusts a potentiometer. Once the dial is set to the desired delay time (between 0 and 20 h), the user pushes a button to set the timer. The timer board responds by flashing the button's internal lamp a number of times equivalent to the delay time in hours, and then entering a sleep mode that consumes less than 1 mA of current. Once satisfied with the chosen delay time, the user disconnects the programming box and installs the hydrophone. The camera is then deployed, and the circuit board wakes up every 10 s to update the internal countdown. Once the countdown is complete, the board powers up the camera through the dock connector, and the One Button mode of the camera is used to start recording upon power up. Subsequent audio and video data are stored as sequential 11 min, 38 s long MP4 files.

Once the camera is activated and recording, the timer board feeds hydrophone audio into the camera's right and left external microphone channels. Hydrophone audio is directly fed to the right channel and is recorded at an effective bandwidth of approximately 15 kHz (100 to 15 000 Hz for MP4 audio). The camera's left channel is fed hydrophone audio that has been heterodyned lower in frequency (referenced to 16 kHz) by a double-balanced mixer, thus accurately recording ultrasonic audio between 17 and 32 kHz. In the ultrasonic channel the hi-pass filter removes components below 16 kHz, while above 32 kHz an anti-aliasing filter engages with a gentle roll off of 20 dB by 40 kHz. (Note: 40 kHz corresponds to the Nyquist frequency of the camera's 48 kHz sampling rate: 16 kHz [heterodyne frequency] + 24 kHz [Nyquist frequency] = 40 kHz.) Thus while intense clicks can generate detectable energy up to 37 kHz, calibrated levels are only available to 32 kHz.

If the signal is fed into the camera at a low level, the automatic gain control is not triggered and the audio can be calibrated; however, this approach yields considerable electronic noise contamination. Subtracting the two audio channels from each other removes most noise contamination while preserving FKW source levels, since both audible and ultrasonic sounds never occurred simultaneously. Unfortunately, the self-noise contamination prevents measurements of the true diffuse ambient background levels from this system, so when estimating detection ranges in Sec. IV, the background noise levels had to be estimated indirectly.

In addition to its timing and hydrophone audio functions, the circuit board also records 3-axis accelerometer data (±2 g full-scale) to a MicroSD card mounted on the board itself [Fig. 2(a)]. The accelerometer (ADXL362) has a sensitivity of 1 mg per bit when set to the 2 g scale. All three acceleration time streams are sampled at 60 Hz and stored in a text file as 12-bit signed integers. The accelerometer begins sampling as the camera awakes, and can continue to log data for over 7 h, even after the camera has shut down.

B. Deployment configuration

Tobias Robinson, a fisherman working with the Southeast Alaska Sperm Whale Avoidance Project, designed a mounting bracket for pelagic mainlines. Two snap-on hooks, identical to those used to attach branchlines to the mainline, were mounted to the assembly to allow rapid attachment and detachment from the 3.5 mm monofilament line. The camera was mounted on the mainline at about 60 m depth, about 10 m from the closest branchline, facing the direction of the fishing vessel [as it hauled gear?] (Fig. 1). As a branchline is also 10 m long, the assembly's elevation angle was set to 45°, which allowed the bait to be centered in the camera's field of view. Branchlines were deployed about 27 m apart, with an estimated uncertainty of ±3 m, given variations in the timing with which the crew attached branchlines during a deployment. No external lighting was permitted due to legal restrictions on fishery operations, so camera operations were restricted to daytime hours.

A NMFS onboard fisheries observer (D.B.) took responsibility for assembling and deploying the camera units. For each deployment the programming time was logged. The sleep interval was typically set between 3 and 4 h, with slightly staggered wake-up times for units deployed on the same set.

C. Source level estimation

After all data had been downloaded, the beginning and end of each video file from every deployment was manually reviewed to determine whether bait or hooked fish had disappeared by the end of the video segment. If so, the time at which a depredation event occurred could be quickly located. Audio data from 30 min before and after a visually observed depredation event were also manually reviewed and annotated using custom MATLAB software. Every whistle was measured for bandwidth, duration, peak power spectral density (PSD), and root-mean-square (rms) sound pressure level (SPL rms). Echolocation clicks were reviewed using 10-s windows. If more than one click was visible within a 10 s window, the most intense click was selected for analysis, in an attempt to limit the potential impact of beam directivity on calculations of the source level. Click received levels only covered the frequency spectrum up to 32 kHz, due to the presence of the gentle anti-aliasing filter above that cutoff frequency. Click durations were computed by measuring the time over which 95% of a signal's cumulative "energy" was attained, with energy defined as the time integral of the difference between the square of the signal's bandpass-filtered pressure and the rms noise level. Whistle durations were measured via manual analysis of spectrograms.

Source levels were estimated by first modeling the transmission loss between the animal and the camera. Historical conductivity, temperature, and depth casts were extracted from the World Ocean Database (WOD), using locations measured in January or February within 1° latitude and 2°

longitude of the camera deployment locations: 19° N and 162° W, respectively. Figure 3 shows the temperature and resulting sound speed profile from a cast collected on January 8, 1989 at 18.0° N, 160° W (WOD Unique Cast Number 11438452). A strong surface duct is visible down to 130 m depth.

The camera's depth was estimated by measuring the travel time of surface-reflected whistle multipath, generated by the animal when it was visible on camera. The time delay was measured by autocorrelating several whistle samples after passing them through a 2 kHz hi-pass finite impulse response filter.

The Gaussian beam ray-tracing program BELLHOP computed the incoherent transmission loss (with a Lloyd's mirror source directionality) between sources placed at 60 m depth (the depth of the depredation event) and receivers placed at various depths between the surface and 1 km. The transmission loss estimates used 5 and 25 kHz as representative frequencies for calculating in-medium (Thorpe) attenuation, as they represent the lower ends of typical FKW whistle and click spectra, respectively. They are the frequency components of whistles and clicks that would suffer the least attenuation during propagation, and thus would be expected to be the frequency components most likely to be detectable over long ranges. A simple logarithmic propagation model (A*$\log_{10}$ Range) was fit to the transmission loss curve between 10 and 500 m range in order to obtain a best-fit value of A, which was found to be 18 for frequencies between 5 and 25 kHz, slightly less than expected from a spherical spreading model due to the existence of the surface duct.

After obtaining this transmission loss law, FKW source levels were estimated two ways. The "direct" method collected a small subset of received levels recorded during and within 10 s of the appearance of an animal on video, and converted them into source level estimates by combining the known ranges of the hooks to the camera with the transmission loss model. The second method took advantage of an unexpected discovery in the acceleration data: a spectrogram analysis of the acceleration time series found that the act of depredating a hook generated a 15–18 Hz 1-s vibration in the mainline. The second "interpolated" method thus estimated source levels for every sound over a 25 min window by deriving the mean speed of the animal along the mainline. This speed was estimated by assuming that these distinctive accelerometer vibrations were indicative of a depredation event off a branchline, and then assuming that the animal depredated the two other hooks preceding the hook in front of the camera (Fig. 1). After estimating the distance between branchlines to be 27 ± 3 m (based on interviews with the skipper), it became possible to derive an average speed by dividing this spacing by the time interval between measured line vibrations. This mean speed was then used to estimate the range of the animal from the camera for every whistle and sampled click by multiplying the mean speed by the time difference between a given acoustic event and the time of the visual sighting. Source levels for all sounds could then be derived from the transmission loss model.

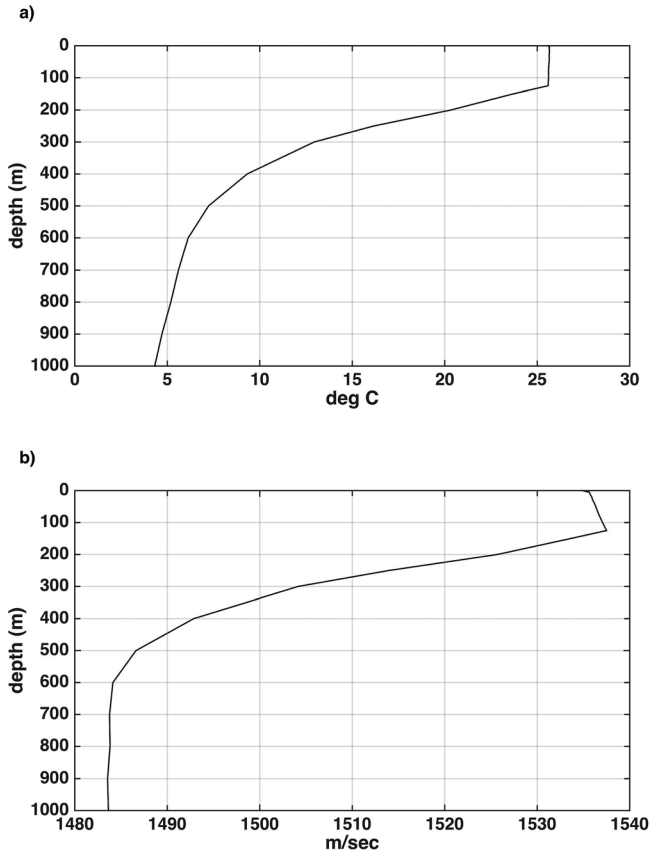

FIG. 3. (a) Historical temperature profile taken from same time of year and geographic location as the depredation encounters, extracted from the WOD. (b) Sound speed profile derived from temperature and concurrent salinity data. Note the presence of a surface duct down to about 130 m depth.

III. RESULTS

A. Description of FKW depredation encounter

Between January 14 and 28, 2015, the F/V *Katy Mary* deployed 14 sets of longline gear, each with 4 Tadpros. Sets 4 and 14 captured video footage of FKW depredation on January 17 and 28, approximately 350 km southeast of Kauai in roughly 5 km deep water. The video from both sets revealed that the animals were taking bait from the hooks and not target fish.

The animal visible in the Set 4 encounter appeared in the video for only a few seconds during depredation, and no sounds were detected during the time the animal was on video, thus precluding the possibility of directly measuring range to acoustic signals. (The lack of coincidence between video and sound also made it difficult to ascertain the camera depth; multipath analysis of an off-screen whistle suggests that the camera was 55 m or deeper.) Furthermore, very few line vibrations associated with depredation could be recognized, possibly due to rough seas and a relative slackness in the mainline. Thus neither the direct nor interpolated methods for estimating source level discussed in Sec. II C were applicable to Set 4, and the acoustic analysis was restricted to Set 14.

TadPro unit 1, which captured the depredation on Set 14, was programmed at 10:07 local time, with a 4 h delay. The depredation was visually recorded between 15:49:24

FIG. 4. (Color online) Image still from FKW depredation video, 15:49:47 on January 27, 2015, using TadPro Unit 1.

and 15:49:54 between roughly 57 to 63 m depth (assuming a 1535 m/s sound speed), and showed a FKW approaching from the direction of the hauling vessel, depredating the bait off the hook (Fig. 4), and then swimming by the camera.

Numerous echolocation clicks and whistles were detected during this 30-s encounter, as well as up to 10 min before and after the videotaped event. The most intense clicks were detected after the depredation, just as the animal begin to swim past the camera. Figure 5 shows some spectrogram examples of whistles detected during the depredation, as well as echolocation clicks directed at the camera.

B. Acceleration and acoustic analysis

Figure 6(a) shows a time-averaged spectrogram of 11 min, 38 s of acoustic data (the length of a GoPro MP4 file) that overlaps the visual depredation encounter (as indicated by the horizontal red line). Both acoustic channels have been subtracted from each other to remove electronic noise, but ultrasonic echolocation clicks dominate the spectrum, so the *y* axis is shown in terms of the ultrasonic channel frequency range. As individual whistles are difficult to see in Fig. 6(a), Fig. 6(b) plots the rms received levels of detected whistles over the same timescale.

Figure 6(c) shows a corresponding spectrogram of the magnitude of the acceleration time series, generated using 256 point-Fast Fourier Transforms (FFTs) with 95% overlap on the 60-Hz sampled data stream. Three prominent line vibrations are noticeable at 15:47:41, 15:48:42, and 15:49:31, roughly a minute apart. Each vibration lasted between 3.4 and 3.8 s and contained maximum spectral intensities between 16.5 and 18.5 Hz. The last vibration was detected when the animal was visible on camera, removing the bait from the hook.

During that same moment an acoustic "rustle" was recorded on the hydrophone, consisting of a 50 ms pulse between 400 and 700 Hz.

We thus interpret these acceleration events as line "plucks" that can be detected on the mainline whenever the line tension is sufficiently high. Given a branch line spacing of roughly 27 m, Fig. 6(c) suggests that line plucks were detected up to 64 m range from the accelerometer, and that the animal was traveling at a speed of 0.54 m/s between the first two hooks and 0.48 m/s between the last two hooks (a mean speed of 0.51 m/s).

Figure 7 shows the subsequent 11 min in the same format as Fig. 6, once the animal had moved past the camera.

C. Source level estimation

Over the two time intervals shown in Figs. 6 and 7, 77 whistles were detected and annotated. Figure 8(a) shows these received whistle intensities over a 25 min span, expressed in terms of both peak PSD and rms value. A whistle can vary in intensity by 10 dB over its duration, so it is unsurprising that whistle rms values are typically 10 dB below their peak PSD values. The red and green (gray in

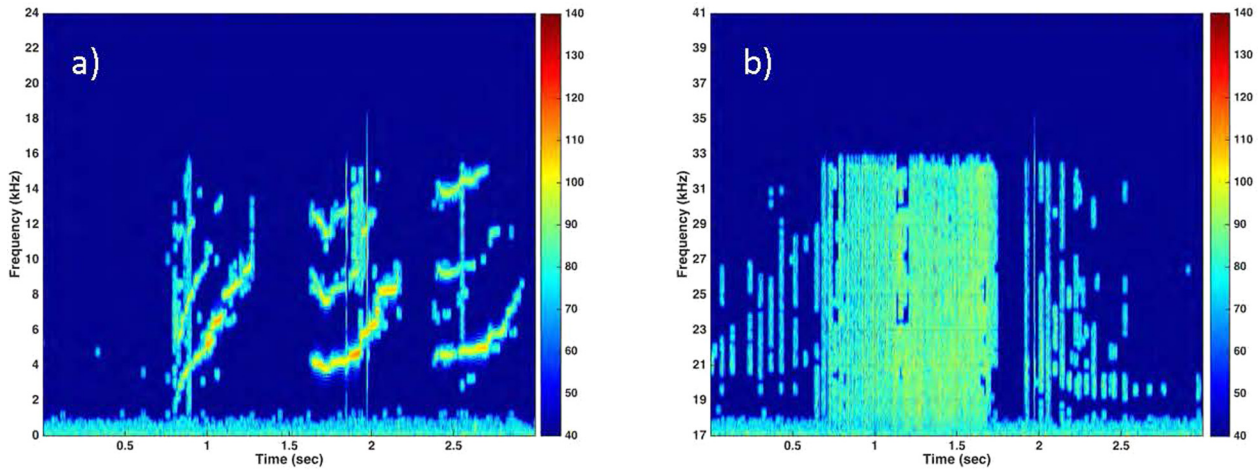

FIG. 5. (Color online) (a) Whistles generated at 15:49:37, a few seconds after depredation. Multipath reflections embedded in this signal yield a recorder depth of about 60 m. (b) Echolocation clicks as animal swims by camera at 15:49:51. The FFT size is 512 points with 90% overlap.

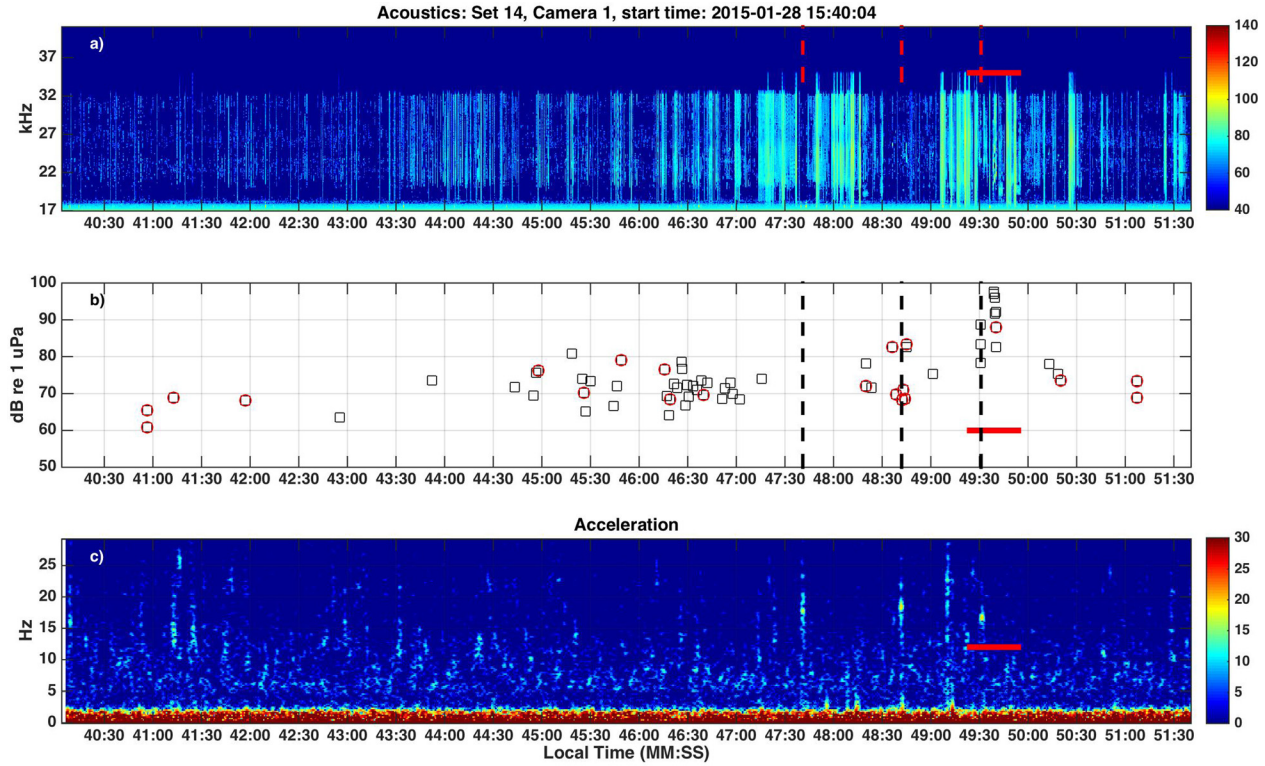

FIG. 6. (Color online) (a) Time-averaged spectrogram of ultrasonic data channel, after differential noise cancellation, between 15:40:06 and 15:51:41, Set 14. The image is generated using a set of 1024-pt FFTs with 75% overlap, averaged over 0.5-s windows before being converted to PSD units of dB re 1 μPa^2/Hz. (b) rms received levels of whistles vs time; whistles with SNRs exceeding 20 dB are plotted as circles. (c) Spectrogram of acceleration magnitude, using 256 pt FFT with 95% overlap. Intensity scale is in units of dB PSD, uncalibrated. Horizontal red lines indicate times when FKW is seen on video. Three 17 Hz vibrations associated with depredation plucks are visible. The vertical dashed lines in (a) and (b) indicate these depredation times.

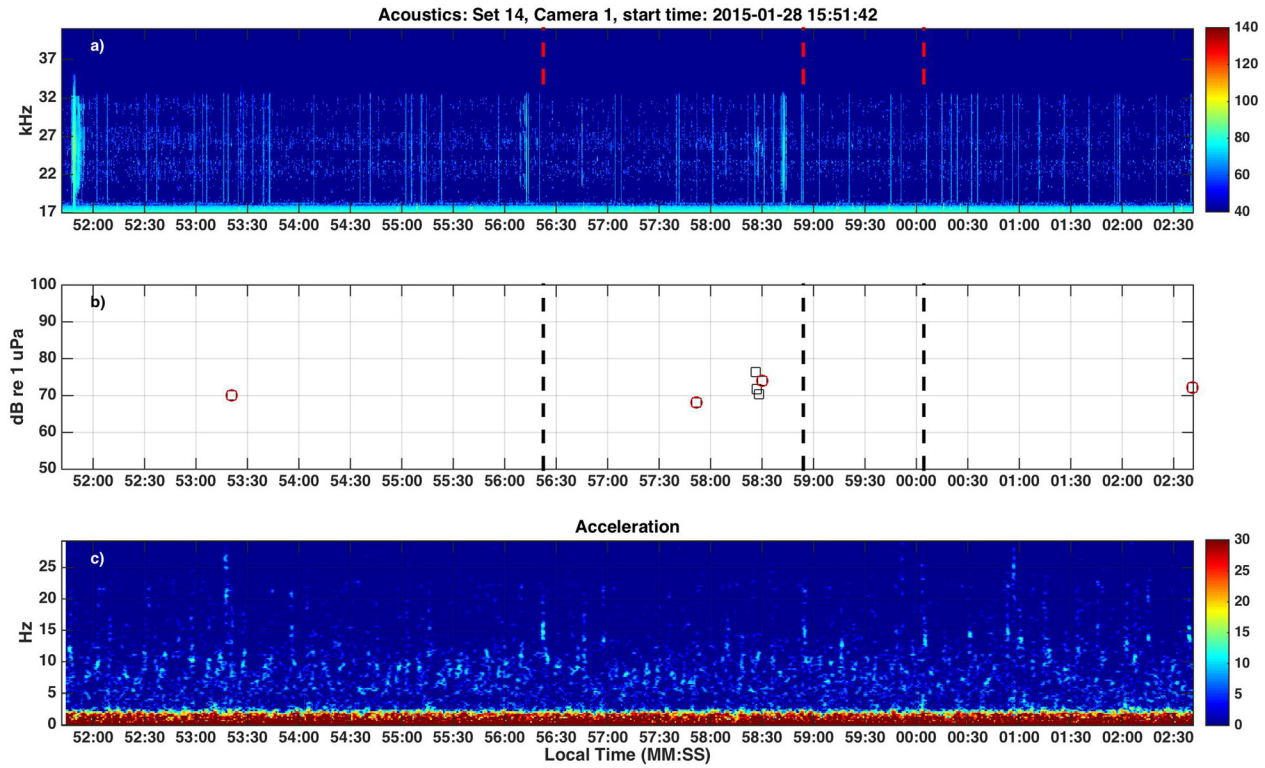

FIG. 7. (Color online) Same format as Fig. 6, but showing 11 min, 38 s of data between 15:51:44 and 16:03:19, after depredation has been caught on camera. Vertical dashed lines in (a) and (b) indicate distinctive line accelerations visible in (c). Numerous line accelerations after 16:00:45 are not marked.

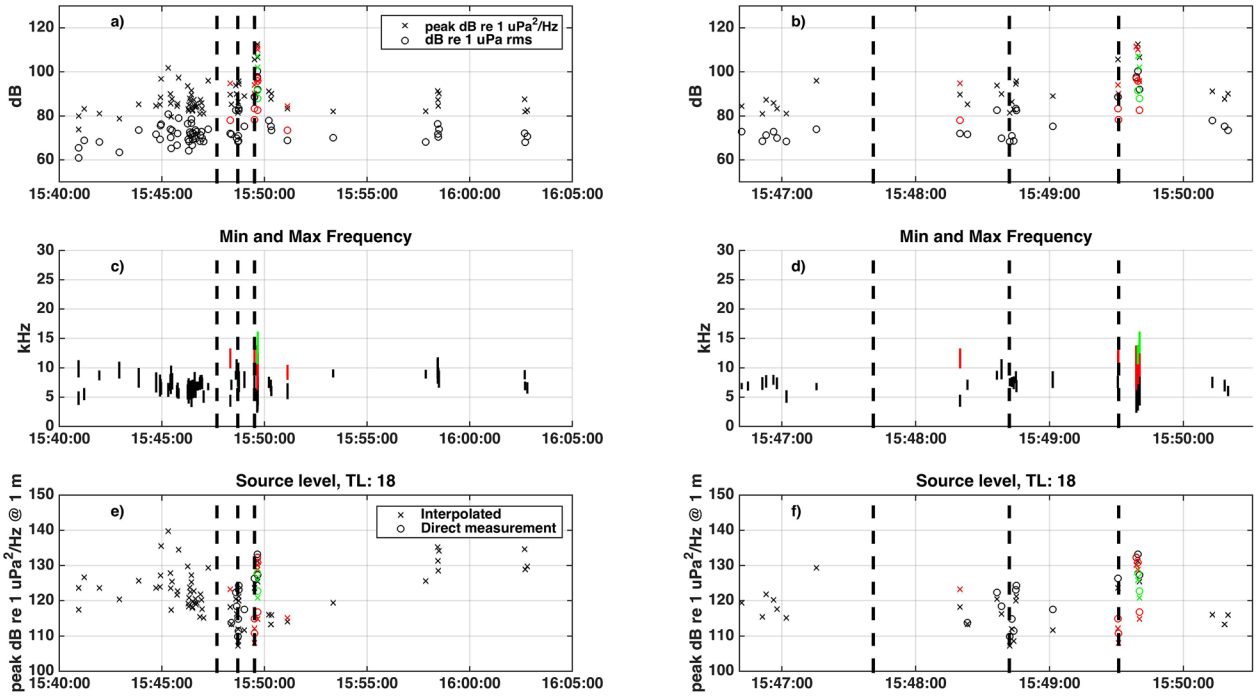

FIG. 8. (Color online) Acoustic properties of whistles. (a) Peak PSD (crosses; dB re 1 μPa^2/Hz) and rms levels (circles; dB re 1 μPa) vs time; (c) whistle bandwidths, where red and green lines and symbols indicate first and second harmonics, respectively; (e) estimated PSD source levels of whistles, using the two approaches discussed in Sec. II C. Vertical dashed lines indicate times of line acceleration. (b), (d), and (f) plot the same data, but are centered on the three depredation events.

black/white) values indicate levels obtained from the first and second harmonics of whistles, which were only present when the whale was depredating in front of the camera [Fig. 4(a)]. Figures 8(c) and 8(d) show the corresponding bandwidths of the whistles (typically 5–8 kHz) and harmonics (red and green [gray in black/white]).

Finally, Figs. 8(e) and 8(f) show the estimated source levels of all the whistles in terms of PSD only and using the 18 log R propagation law derived from Sec. II C. The circles indicate source levels of whistles detected within 10 s of the video encounter, and thus whose range is well established. The crosses show source level estimates obtained by assuming a swimming speed of 0.51 m/s and converting times into slant ranges. The vertical dashed lines indicate times of line plucks; the last such line indicates when the depredation was seen on video.

Figure 9 shows the properties of 103 clicks measured over the same 25-min window as Fig. 8. The received levels in Figs. 9(a) and 9(b) are given in terms of maximum PSD, rms, and peak-to-peak values to facilitate comparisons with previous literature. Figures 9(c) and 9(d) show the bandwidths of the selected signals. All click energy lay in the ultrasonic channel, due to high internal noise levels in the lower-band channel; hence only frequencies above 17 kHz are shown. The click bandwidths in Figs. 9(c) and 9(d) occasionally exceed the 32 kHz design cutoff frequency, due to the gentle roll-off of the anti-aliasing filter discussed in Sec. II A.

Figures 9(e) and 9(f) use a 18 log R propagation loss law (derived for a 25 kHz signal in Sec. II C) to obtain the corresponding source level estimates in 3 different dB units. The exact interval between branch lines was unimportant to the final result: the source level estimates remained virtually unchanged if branch line intervals were varied between 24 and 30 m.

Figures 9(e) and 9(f) use a 18 log R propagation loss law (derived for a 25 kHz signal in Sec. II C) to obtain the corresponding source level estimates in 3 different dB units. The exact interval between branch lines was unimportant to the final result: the source level estimates remained virtually unchanged if branch line intervals were varied between 24 and 30 m.

IV. DISCUSSION

A. Comparison with previous literature

The source levels reported here are "apparent" source levels (ASL; Madsen *et al.*, 2004), in that they represent off-axis measurements of the source intensity, and thus do not represent the source levels one would obtain for measurements made within the animals' on-axis sonar beam, such as presented in Madsen *et al.* (2004) or Kloepper *et al.* (2012). ASLs are appropriate choices for estimating passive acoustic detection ranges of these sounds, as the probability of capturing an on-axis sound from a distant animal is low.

Whistle source levels in Figs. 8(e) and 8(f) have been expressed only in terms of PSD instead of broadband SPL rms, because PSD is the more relevant quantity for estimating detection range; the rms value would underestimate detection range because the dynamic range of a whistle's intensity is so large that components of the whistle can exceed the rms value by 10 dB [per Figs. 8(a) and 8(b)]. Furthermore, rms levels depend on the whistle's duration, which tends to decrease with range, as the beginning and

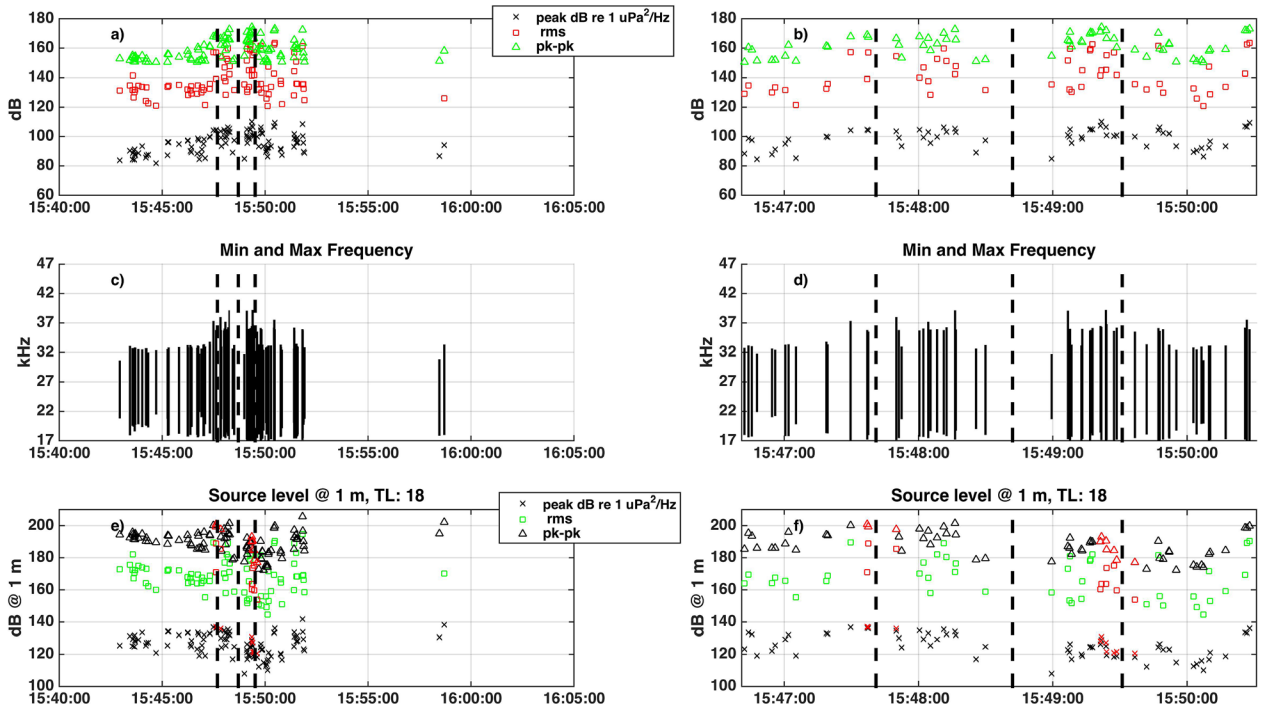

FIG. 9. (Color online) Acoustic properties of echolocation clicks between 17 and 32 kHz bandwidth. (a) Received levels (dB) in terms of peak PSD (crosses; dB re 1 μPa^2/Hz), rms (squares; dB re 1 μPa), and peak-to-peak (triangles; dB re 1 μPa). (c) Click bandwidths; (e) estimated source levels using same symbols as (a). Vertical dashed lines indicate times of line acceleration. (b), (d), and (f) plot the same data, but are centered on the three depredation events.

end of a whistle tend to have lower intensities than the middle.

The 190–200 dB pk-pk levels reported here for clicks are 10 dB lower than what has been reported in Madsen *et al.* (2004), and the 170–180 rms levels are 20 dB lower than the rms levels reported in the same paper; however, the results here are limited to frequency components below 30 kHz, while Madsen *et al.* (2004) measured clicks over a much broader bandwidth. Unfortunately, Madsen *et al.* (2004) neither published source PSD levels nor published the characteristics of off-axis clicks that would permit more direct comparisons with the work conducted here.

B. Observations of acoustic behavior

An odd result apparent from Figs. 6–9 is that shortly after the animal passed the camera much lower rates of acoustic activity were detected in terms of both whistles and clicks. For example, Fig. 8(a) shows how whistle detection rates dropped substantially once the animal passed the camera (15:49:31). A natural explanation would be that the directivity of both clicks and whistles are large, so that sounds detected behind a swimming animal generally would have much lower received levels than sounds detected on approach. The few clicks and whistles visible in Figs. 8(e) and 9(e) would then be interpreted as relatively rare moments when the animal has oriented its head back toward the vessel. Au *et al.* (1995) measured click beam directivities between 22 and 29 dB, depending on frequency, a contrast in apparent source levels that is consistent with what has been observed here. No published data on the directivity of FKW whistles has been located, but Miller (2002) observed some evidence of whistle directivity in resident killer whales.

A comparison of the timing of acoustic and acceleration events suggests that sets of echolocation clicks may occur just before line accelerations. Two of the three line accelerations marked in Fig. 6(a) are preceded by click bursts, and Fig. 7(a) shows two additional line accelerations between 15:51 and 16:03 that are associated with click bursts 10–15 s before the hypothesized depredation events. Whistles are also detected within the 30 s preceding line accelerations in 4 out of the 6 acceleration events marked in Figs. 6 and 7.

C. Estimated detection ranges of FKW whistles and clicks

One practical application of these source level estimates is that they can be used to estimate the passive acoustic detection range of FKW whistles as a function of sea state, where "sea state" refers to the definition used by Wenz (1962), which roughly corresponds to one less than the Beaufort wind scale. This detection range can be estimated provided that (a) the signal transmission loss can be computed as a function of source depth and range, (b) representative background ambient noise levels can be estimated, and (c) a minimum signal-to-noise ratio (SNR) for detectability can be assumed. Section II C has already addressed the first requirement, and the resultant Fig. 10 displays the transmission loss estimates for 5 and 25 kHz signals for a 60 m deep source (the depth of the camera for Set 14) as a function of receiver range and depth, using the sound speed profiles shown in Fig. 3. The propagation enhancement arising from the surface duct is readily visible in both figures; at a fixed range propagation can be enhanced by up to 10 dB by placing the receiver at depths shallower than 130 m, provided that the source is also shallower than that depth.

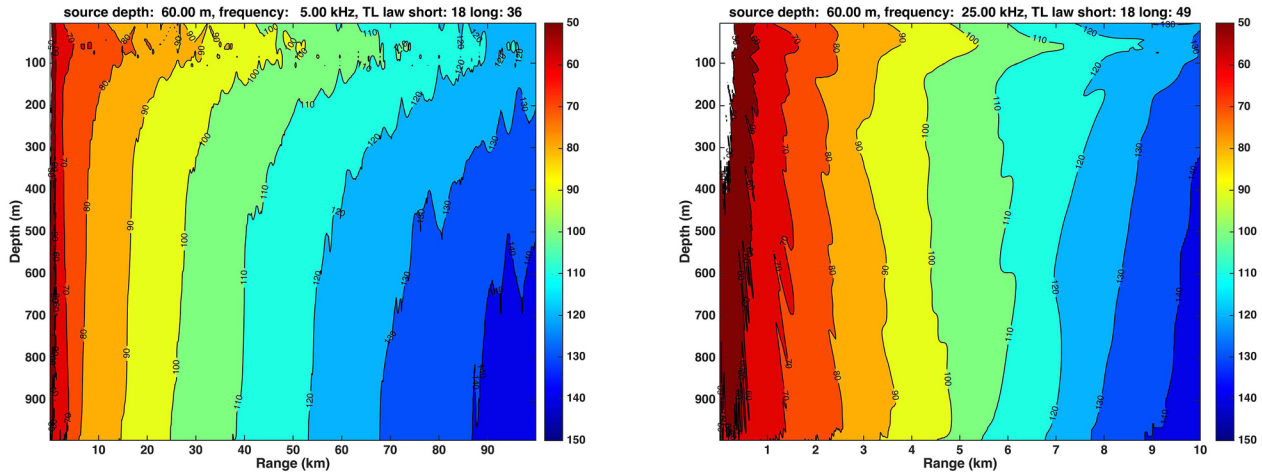

FIG. 10. (Color online) Computed transmission loss of (a) 5 kHz and (b) 25 kHz signals using the sound speed profile in Fig. 3 and assuming a source depth of 60 m. Note the different range scales for both figures: the 25 kHz signal attenuates much more rapidly with range than the 5 kHz signal due to increased bulk water attenuation.

The second requirement—estimating representative background noise levels—is more problematic in that the electronic self-noise levels on the GoPro instruments precluded accurate acoustic ambient noise level estimates, and that the fishing logs did not note the local weather. To obtain a representative example of the background noise levels present during the longline haul, Advanced SCATterometer (ASCAT) measurements from the European Space Agency's METOP-A and METOP-B meteorological satellites were used to estimate surface wind speeds on the same date as and near to the camera deployments, using the Ocean Surface Winds Team databases provided by the NOAA/NESDIS Center for Satellite Applications and Research. Wind speeds were translated to sea state ratings as defined in Wenz (1962). That same reference was then used to convert sea state into predictions of deep-water ambient noise levels as a function of frequency. Thus METOP-A ASCAT measurements from January 28 (Set 14 haul) show 15–20 knot winds in the area, which translates into an expected sea state of 4. At 5 kHz Wenz (1962) predicts a wind-driven background noise PSD of 50 dB re 1 μPa^2/Hz, which decreases to 47 dB as the acoustic frequency increases to 10 kHz.

Combining all this information, and assuming that a SNR of 5 dB is detectable by a human monitor, one finds that at sea state 4 the 120–130 dB re 1 μPa^2/Hz whistle PSD source levels shown in Fig. 8(b) would fall to 55 dB re 1 μPa^2/Hz after experiencing a 65–75 dB transmission loss, which occurs at ranges between 2 and 10 km for the optimal 60 m receiver depth [Fig. 10(a)]. Under calmer conditions (sea state 1) background noise levels would fall to 40 dB re 1 μPa^2/Hz at 5 kHz, allowing peak transmission losses of 75–85 dB, with corresponding maximum detection ranges of 10–25 km for a 60 m deep sensor. The exact depth of the source only becomes important if it is placed below the 130 m deep thermocline; for example, a 400 m depth source will have a 10 dB higher transmission loss at a fixed range than a 60 m depth source, reducing the detection range from 25 to 10 km for a 60 m deep sensor in sea state 1 conditions.

Thus during very calm sea states intense FKW whistles might produce at least 5 dB SNR signals on a 60 m deep sensor over ranges that would span most of a 60-km pelagic longline deployment, provided that the sensor were placed midway on the set, and that no fishing vessel were nearby. However, a single 60 m deep hydrophone deployed by a drifting, silent, fishing vessel checking for moderately intense FKW whistles before a deployment would be likely only to monitor between 2 km (sea state 4) to 10 km (sea state 1) range, assuming a 5 dB signal-to-noise detection ratio and for animals calling above the thermocline. In order to monitor locations 60 km away before a deployment, a hypothetical passive acoustic system would need a minimum array gain of 20 dB to detect shallow and strong FKW whistles in even the calmest sea states (sea state 1). Were the ambient noise field completely nondirectional, a 100 hydrophone array with 15 m aperture would be needed to monitor this distance. In reality the ambient noise field may have a fairly high directionality, so fewer hydrophones might be required to attain the needed gain.

Echolocation clicks cannot be detected at greater ranges than whistles, due to their higher absorption losses at higher frequencies. At sea states 1 and 4 the expected ambient background noise levels at 25 kHz would be 32 and 42 dB re 1 μPa^2/Hz, respectively (Wenz, 1962), so given a 130 dB PSD click source level at this frequency and 5 dB required SNR, the largest permitted transmission losses would be 93 dB at sea state 1 and 83 dB at sea state 4, which occur at respective ranges of 4.2 and 3 km in Fig. 10(b).

Madsen *et al.* (2004) found that the peak PSD of echolocation clicks is around 6 dB greater at 40 kHz than at the 25 kHz level measured here. Repeating the above calculations with appropriate transmission loss modeling and ambient noise levels finds a maximum possible detection range of 3 km for a 5 dB SNR 40 kHz signal at sea state 1. Therefore, even though ambient noise levels are lower and the source levels higher at 40 kHz, the associated transmission losses are much greater, and the 25 kHz click components measured by the TadPro are the components that would be detected at the greatest distances (e.g., 4.2 km at sea state 1). The predictions of this analysis are thus consistent with the spectral measurements of Baumann-Pickering *et al.* (2015),

which used fixed bottom-mounted recorders to find that both FKW and short-finned pilot whale clicks detected at unknown ranges of a few kilometers tended to have broad peaks at the lower end of the click spectrum (22–25 kHz). Note that the detection distance for the lowest-frequency click components is still at least 5 times smaller than the 25 km detection range of a 130 dB re 1 μPa^2/Hz whistle at sea state 1.

V. CONCLUSION

Simultaneous measurements of video, acoustic, and line vibration collected during a FKW depredation event have shown that the animals are depredating bait, and that they are acoustically active even during daylight hours under good visual conditions. The combined sensory data have been used to estimate source levels of both a FKW's whistles and the lower bandwidth of its echolocation clicks, which in turn has permitted the detection range of these signals to be estimated as a function of sea state and animal depth. This information would be useful in evaluating what role passive acoustic monitoring could play in observing and reducing depredation encounters, and some simple calculations have been presented in the Discussion. The greatest uncertainty remaining in estimating detection range to these animals is a lack of knowledge of the vertical directionality of the wind-driven ambient noise field at the fishing grounds.

The possibility that depredation may generate distinctive line accelerations is intriguing in that it raises the possibility that small, inexpensive off-the-shelf acceleration loggers could be used to identify depredation rates, provided that accelerations associated with depredation can be distinguished from accelerations arising from the hooking of target or other bycatch species. The fact that FKWs will consume bait on hooks (as well as target fish) suggests that the scale of depredation activity by FKWs may be undercounted; for example, evidence for bait depredation is likely underestimated in NOAA observer protocols. The use of both acceleration and acoustic measurements may provide useful tools to estimate the magnitude of depredation efforts on this fishery. The lack of clear depredation signatures in the acceleration data for Set 4 indicates that more analysis is needed to understand the circumstances under which depredation-based line vibrations are generated and detected.

ACKNOWLEDGMENTS

The authors are indebted to Captain Jerry Ray and the rest of the F/V Katy Mary crew for permitting the camera gear to be deployed during their longline fishing trip. Robert Glatts designed the custom GoPro circuit board, and Will Cerf assisted with video footage analysis. This research was sponsored by Derek Orner under the Bycatch Reduction Engineering Program (BREP) at the National Oceanic and Atmospheric Administration (NOAA).

Au, W. W., Pawloski, J. L., Nachtigall, P. E., Blonz, M., and Gisner, R. C. (**1995**). "Echolocation signals and transmission beam pattern of a false killer whale (*Pseudorca crassidens*)," J. Acoust. Soc. Am. **98**, 51–59.

Baumann-Pickering, S., Simonis, A. E., Oleson, E. M., Baird, R. W., Roch, M. A., and Wiggins, S. M. (**2015**). "False killer whale and short-finned pilot whale acoustic identification," Endangered Species Res. **28**, 97–108.

Bayless, A. R., Oleson, E. M., Baumann-Pickering, S., Simonis, A. E., Marchetti, J., Martin, S., and Wiggins, S. M. (**2017**). "Acoustically monitoring the Hawai'i longline fishery for interactions with false killer whales," Fisheries Res. (in press).

Bradford, A. L., and Forney, K. A. (**2016**). "Injury determinations for marine mammals observed interacting with Hawaii and American Samoa longline fisheries during 2009-2013," U.S. Department of Commerce, NOAA Tech. Memo., NOAA-TM-NMFS-PIFSC-50, 54 pp.

Brill, R. L., Pawloski, J. L., Helweg, D. A., Au, W. W., and Moore, P. W. B. (**1992**). "Target detection, shape-discrimination, and signal characteristics of an echolocating false killer whale (*Pseudorca crassidens*)," J. Acoust. Soc. Am. **92**, 1324–1330.

Carretta, J. V., Oleson, E. M., Baker, J., Weller, D. W., Lang, A. R., Forney, K. A., Muto, M. M., Hanson, B., Orr, A. J., Huber, H., Lowry, M. S., Barlow, J., Moore, J. E., Lynch, D., Carswell, L., and Brownell, R. L., Jr. (**2016**). "US Pacific marine mammal stock assessments, 2015," NOAA-TM-NMFS-SWFSC-561.

Gilman, E., Brothers, N., McPherson, G., and Dalzell, P. (**2007**). "A review of cetacean interactions with longline gear," J. Cetacean Res. Manage. **8**, 215–223.

Hamer, D. J., Childerhouse, S. J., and Gales, N. J. (**2012**). "Odontocete bycatch and depredation in longline fisheries: A review of available literature and of potential solutions," Marine Mammal Sci. **28**, E345–E374.

Kloepper, L. N., Nachtigall, P. E., Donahue, M. J., and Breese, M. (**2012**). "Active echolocation beam focusing in the false killer whale, *Pseudorca crassidens*," J. Exp. Biol. **215**, 1306–1312.

Madsen, P., Kerr, I., and Payne, R. (**2004**). "Echolocation clicks of two free-ranging, oceanic delphinids with different food preferences: False killer whales *Pseudorca crassidens* and Risso's dolphins *Grampus griseus*," J. Exp. Biol. **207**, 1811–1823.

Miller, P. J. O. (**2002**). "Mixed-directionality of killer whale stereotyped calls: A direction of movement cue?," Behav. Ecol. Sociobiol. **52**, 262–270.

Oswald, J. N., Barlow, J., and Norris, T. F. (**2003**). "Acoustic identification of nine delphinid species in the eastern tropical Pacific Ocean," Marine Mammal Sci. **19**, 20–37.

Thomas, J., Stoermer, M., Bowers, C., Anderson, L., and Garver, A. (**1988**). "Detection abilities and signal characteristics of echolocating false killer whales (*Pseudorca crassidens*)," in *Animal Sonar* (Springer, New York), pp. 323–328.

Watson, J., and Kerstetter, D. (**2006**). "Pelagic longline fishing gear: A brief history and review of research efforts to improve selectivity," Mar. Technol. Soc. J. **40**, 6–11.

Wenz, G. M. (**1962**). "Acoustic ambient noise in the ocean: Spectra and sources," J. Acoust. Soc. Am. **34**, 1936–1956.

www.groupbinc.com (Last viewed October 21, 2016).